AeroBest 2025
Lisboa, 22–24 April 2025
©ECCOMAS, Portugal

IMPACT OF ADOPTING ACTIVE FLUTTER SUPPRESSION SYSTEMS ON THE OPTIMIZATION OF A TYPICAL LONG-RANGE TRANSPORT AIRCRAFT

Elena Roncolini*, **Francesco Toffol and Sergio Ricci**

Department of Aerospace Science and Technology
Politechnico di Milano
Via La Masa 34, Milano - ITALY

*elena.roncolini@polimi.it, http://www.aero.polimi.it

{francesco.toffol, sergio.ricci}@polimi.it, http://www.aero.polimi.it

Abstract. *The increasing pressure to reduce the environmental impact of future aircraft is driving the adoption of more innovative aerostructural solutions, such as unconventional configurations and the use of active control systems to ensure high overall efficiency across the entire flight envelope. Implementing high aspect ratio wings to decrease induced drag, which are generally more flexible, requires advanced active control systems to mitigate potential aeroelastic issues. Active Wing Control systems are likely to be integrated with technologies currently utilized in existing fly-by-wire control systems. However, Active Flutter Suppression systems (AFS) are relatively new, although with a long history behind them, and their expected performance and technical feasibility need to be evaluated in terms of safety, robustness, and reliability. Despite this, two aircrafts with AWC have been certified under special conditions: the B747-800 and the B787-10, highlighting the necessity for further investigation into the adoption and certification of these systems. Setting aside the intricate certification considerations, a key design question remains: assuming stability can be assured with suitable AFS systems, what potential weight savings could be achieved by designing the structure without the explicit constraint of a minimum flutter velocity requirement? This paper focuses on a generic long-range, twin-aisle transport aircraft and presents comparisons based on optimizing the wing structure with various design constraints, including or excluding the flutter constraint, to draw general conclusions.*

Keywords: Active Flutter Suppression (AFS), aeroelastic optimization

1 INTRODUCTION

Flutter is a dynamic aeroelastic instability that can lead to divergent oscillatory vibrations, posing a significant risk to aircraft performance and safety, potentially resulting in aircraft loss [1]. In the traditional three-phase design process - conceptual, preliminary, and detailed - flutter analysis is typically conducted once a sufficiently accurate aeroelastic model is available [2]. However, conventional conceptual design tools often rely on statistical methods that are unable to accurately capture unsteady aerodynamic and structural stiffness effects, limiting their efficacy in flutter prediction [3].

In industrial practice, flutter analysis is usually performed once the Global Finite Element Model (GFEM) of the aircraft is developed. This model facilitates the creation of a reduced structural representation (stick model) for flutter calculations within the modal space [4]. If the design fails to meet flutter requirements, redesign efforts become necessary, often leading to increased costs and extended development timelines.

To mitigate these challenges, integrating flutter analysis early in the aircraft design process - particularly in wing design - can streamline development by enabling more informed trade-offs between flutter constraints, performance objectives, and other design considerations. Therefore, there is growing interest in incorporating flutter constraints into standard Multidisciplinary Design Optimization (MDO) frameworks [5]. This approach allows for the simultaneous optimization of aerodynamic and structural parameters, enabling structural weight and fuel consumption minimizations, while ensuring compliance with flutter requirements [6].

Despite ongoing research, integrating flutter constraints into optimization cycles remains a challenge [3]. Flutter is inherently complex and nonlinear, though often linearized for practical purposes, making it difficult to express it as an explicit constraint [7]. The computational model must balance complexity, being detailed enough to capture critical aeroelastic effects while remaining efficient for iterative design processes [8, 9]. Additionally, optimization methodologies vary widely, encompassing gradient-based and other methods, integer and continuous variables, and local versus global solution strategies.

Further considerations involve the inclusion of post-flutter behavior as a design requirement [10], or the role of Active Flutter Suppression (AFS) systems. While various AFS solutions have been explored over the years, certification regulations have historically adopted a conservative stance, prohibiting the certification of aircraft exhibiting flutter within the flight envelope, due to safety concerns [11].

Recently, two key developments have renewed interest in these topics.

First, the push for reduced environmental impact in future civil aircrafts has led to the exploration of unconventional and innovative configurations. High Aspect-Ratio Wings (HARW), designed to minimize induced drag during cruise, exhibit significant structural flexibility, making them more susceptible to aeroelastic phenomena, including flutter and associated nonlinearities [12]. Moreover, many proposed configurations incorporate distributed or unconventional propulsion systems, leading to an increased modal density in the wing structure compared to traditional designs. These challenges must be addressed from the earliest design stages.

Second, for the first time in years, there is recognition of the need to update certification processes to accommodate active flutter mitigation or suppression systems. Rather than being seen solely as a corrective measure for unexpected flutter behavior discovered during certification, AFS is now being considered a fundamental design opportunity.

Active Wing Control (AWC) systems are likely to be integrated with technologies currently utilized in existing fly-by-wire control systems. However, AFS are relatively new, although they have a long history behind them [1], and their expected performance and technical feasibility need to be evaluated in terms of safety, robustness and reliability. Despite this, two AWC aircrafts have been certified under special conditions: the B747-800 and the B787-10 (see [13, 14]), highlighting the need for further investigation into the adoption and certification of these systems.

Recent research efforts have focused on the actuation, detection, redundancy, and validation aspects of AFS. The main objective is to confirm the feasibility of these systems in addressing unforeseen situations that arise during the final design phase, where they become the sole systems ensuring the minimum aeroelastic damping required for successful certification. Essentially, AFS systems are designed to rectify unintentional instability cases that cannot be resolved otherwise.

Setting aside the intricate certification considerations, a key design question remains: assuming stability can be assured with suitable AFS systems, what potential weight savings could be achieved by designing the structure without the explicit constraint of a minimum flutter velocity requirement?

This paper focuses on a generic long-range, twin-aisle transport aircraft and presents comparisons of wing structure optimizations with various design constraints, including or excluding flutter, to draw general conclusions. Exploring the integration of flutter constraints in modern aircraft design and optimization methodologies, the present work does not answer completely the many open issues, but it wants to open the discussion among the researchers in the field.

2 USED TOOLS

Recognizing the importance of integrating aeroelastic considerations from the initial design phase - particularly given the increasing flexibility of modern aircrafts - POLIMI started developing the NeoCASS design suite in 2007 [15–17]. NeoCASS was among the first physics-based conceptual design tools, aiming to provide:

1. a simplified yet realistic structural model, capable of capturing key aeroelastic characteristics through rapid analyses;
2. automated structural model generation, seamlessly integrated into conceptual design workflows;
3. a transparent user experience, minimizing the need for expertise in finite element and aeroelastic analysis.

NeoCASS employs a simplified finite element model - stick model with beam elements - along with a Vortex Lattice (VLM) or Doublet Lattice (DLM) model for steady and unsteady calculations, respectively.

Beyond the aeroelastic predictive capabilities, the early use of stick finite element models is mainly what diversifies NeoCASS from conventional industrial approaches. Indeed, while in industry one typically relies on statistical mass estimates during conceptual design only introducing a GFEM, after selecting candidate configurations, NeoCASS integrates structural sizing from the outset. By using stick models for the full load set required by certification regulations, it offers physics-based structural weight estimation, eliminating reliance on statistical data often unavailable for novel technologies or unconventional aircraft configurations and aligning with aeroelastic requirements. The minimum structural mass is then determined solely by the material required to sustain applied loads. This contrasts with traditional workflows, where aeroelastic assessments occur late in the process, often necessitating design revisions that lead to weight penalties.

Over the past decade, several conceptual and preliminary design tools have emerged, including PROTEUS (TU-Delft), ATLASS (Gulfstream), Bombardier's proprietary methodology, and EMWET, among others. Many of them depend on GFEMs or commercial finite element software, limiting their applicability at the conceptual design stage, where hundreds or thousands of configurations must be evaluated. Differently, NeoCASS automatically generates stick models at the beginning of the design loop from a limited set of geometric inputs, sizing the aircraft based on real load conditions dictated by certification rules (e.g., CS23, CS25) [18, 19]. As anticipated, this approach enables a realistic mass and stiffness distribution for structural elements, while relying on statistical models for non-structural masses.

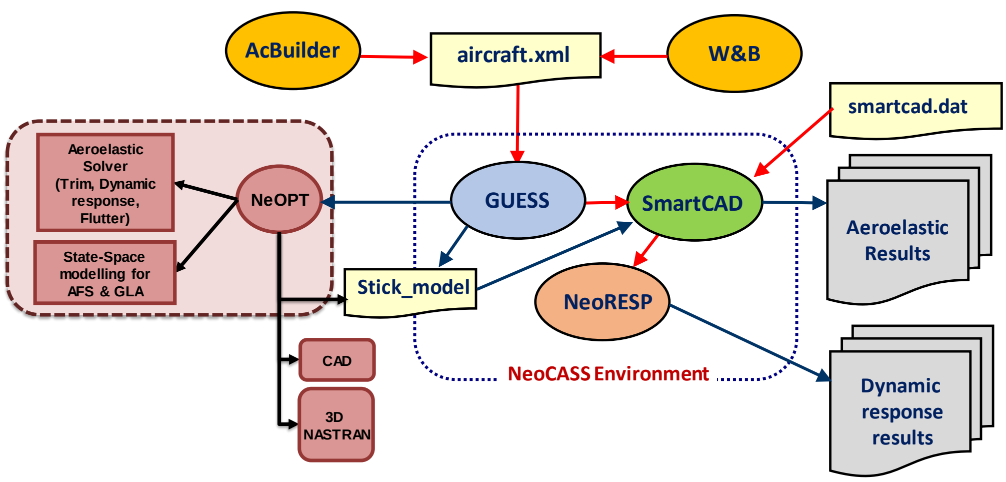

Figure 1: NeoCASS Overview

To accelerate the automatic sizing process, NeoCASS incorporates simplifications, limiting structural models to isotropic or quasi-isotropic materials (e.g. composites are treated as "black aluminum"). This restricts the ability to capture fiber-induced structural coupling. Additionally, for unconventional configurations like Blended-Wing Bodies (BWB) or Strut-Braced Wings (SBW), a beam-only model cannot fully capture structural behavior, necessitating 3D modeling capabilities. To address these issues, NeoCASS underwent a major revision, introducing the NeOPT optimization module and enhancing solvers, particularly for composite wing structures. The integration of NeoCASS and

NeOPT creates a unified design suite, where wingbox sizing is conducted via a semi-analytical meta-model representation. This enables comprehensive structural and aeroelastic assessments, including failure and buckling analyses, flutter, control effectiveness, and gust response - with and without active control technologies (e.g. maneuver and gust load alleviation systems) [20, 21].
Figure 1 provides a schematic overview of NeoCASS, which consists of three core modules:

1. GUESS: performs initial structural sizing based on limited geometric inputs and user-selected structural design philosophy. The sizing process adheres to certification rules or user-defined maneuver sets.

2. SmartCAD: the aeroelastic kernel, comprising solvers for aeroelastic trim, flutter, and control reversal analyses. Both GUESS and SmartCAD employ frozen maneuvers to solve trim problems algebraically, without time-dependent load evolution.

3. NeoRESP: solves generic response problems, including frequency-domain gust response analysis and state-space model generation for active control system design, such as maneuver and gust load alleviation systems.

The code includes two additional modules: AcBuilder, for parametric aircraft geometry definition; Weight & Balance (W&B), for initial mass estimation via statistical formulas. The latter provides a preliminary mass distribution, which serves as an input for structural sizing in GUESS. A simplified but complete finite element aeroelastic model, supported by dedicated structural and aerodynamic solvers, is then generated. The structural model relies on a nonlinear three-node finite volume beam approach, while aerodynamic computations leverage Vortex Lattice and Doublet Lattice methods for steady and unsteady conditions, respectively.

In summary, GUESS enables a physics-based, fully stressed aircraft design with key simplifications to expedite the process and facilitate automatic aeroelastic model generation. These include assuming a rectangular and symmetric wingbox, limiting materials to isotropic types, conducting rigid trim-based load envelope analyses, and omitting direct load sensitivity calculations with respect to design variables. These challenges are then addressed by the new NeOPT module, which refines the wingbox sized by GUESS by means of optimization. A Meta-Model approach is adopted, with a semi-analytical representation of the wingbox that organizes its 3D geometrical and physical properties into a unified framework. This allows different analysis models to be managed using a single set of information, enabling seamless result transfer between domains. The wingbox is modeled with higher fidelity without increasing FEM model complexity. Additionally, the sizing process leverages all NeoCASS solvers, incorporating dynamic load conditions such as gusts and control inputs, as well as flutter analysis to ensure the aero-servo-elastic stability of the aircraft.

In this paper, NeoCASS and NeOPT have been coupled in an integrated MDO framework tailored for flutter optimization of a typical long-range transport aircraft.

3 FLUTTER OPTIMIZATION AND CERTIFICATION RULES

The FAA Part 25 (Title 14, Code of Federal Regulations Part 25) [22] and EASA CS-25 (Certification Specifications for Large Aeroplanes) [18] contain specific requirements related to stability, control, and flutter for commercial transport aircrafts. From the stability and flutter perspective, the key certification requirements include the following:

- the aircraft must be free from aeroelastic instability (flutter, divergence, control reversal) for all speeds up to 1.15 times the dive speed (V_D).
- Flutter clearance must be demonstrated considering structural damping, aerodynamic forces, and mass properties.
- Damping requirements: all aeroelastic modes must be sufficiently damped across the entire flight envelope.
- Mass balancing of control surfaces must prevent flutter.
- Ground Vibration Testing (GVT) and analytical validation are required to confirm that the structural and aerodynamic models accurately predict flutter behavior.

The same requirements can be coded in a graphical way in what is called Method 1, where no structural damping is included in the model before computing flutter analysis:

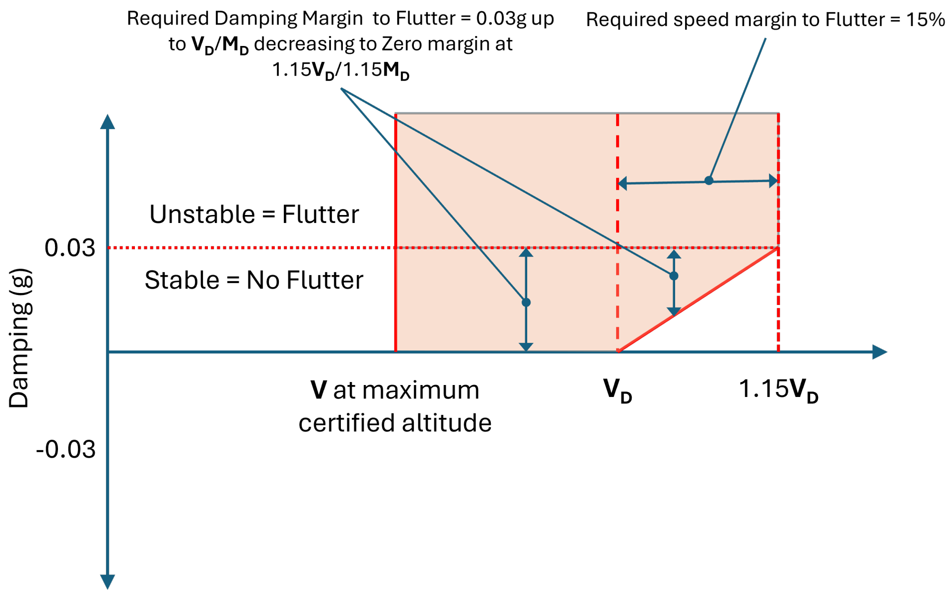

Figure 2: Method 1 - flutter requirements in shaded region

By analyzing Figure 2, we can determine that the aircraft exhibits natural or passive stability and complies with CS-25 regulations if a damping margin of g=0.03 is guaranteed up to V_D, and linearly reduced up to 1.15 V_D. Flutter stability is hence guaranteed if the tracked modal dampings do not cross g=0 line up to V_D and g=0.03 line up to 1.15 V_D. This is valid in case no structural damping is included in the model.

The literature presents various examples of aeroelastic optimization with flutter constraints, implemented using different minimization algorithms, such as gradient-based and stochastic methods, but all adhering to the same regulatory requirements in different ways. Some studies apply an explicit constraint on velocity or minimum damping values, while others impose broader constraints on entire rejection curves to prevent potential hump modes from entering the rejection zone [23, 24].

It is important to note that in a more realistic nonlinear approach, flutter constraints can vary with flight parameters, as they depend on the specific conditions at which the problem is linearized. Traditionally, to achieve a balance between computational cost and accurate problem representation, flutter constraints are often imposed in frequency domain. This is done by coupling medium-complexity finite element structural models with unsteady aerodynamic methods, typically analyzed using the Doublet-Lattice Method (DLM).

The approach of designing a naturally or passively flutter-free aircraft relies primarily on optimizing the distribution of stiffness and mass along the wing, demonstrating analytically - then experimentally - that the imposed regulatory conditions are satisfied.

Interest in AFS systems, which ensure the necessary damping through active control technologies, has long captured the imagination of researchers. Since the late 1970s, various solutions have been proposed, transitioning from purely passive optimization to hybrid, or aeroservoelastic, optimization. Nontheless, this approach has never been a viable design option due to regulatory limitations, as well as concerns regarding safety and robustness [12].

As anticipated, the situation has recently evolved due to two key factors: the drive for more efficient, lighter aircrafts and the certification of two aircrafts that seemingly contradict the traditional principle of flutter-freedom up to 1.15 V_D, without relying on dedicated active control systems. Specifically, the cases at hand are Boeing 747-800 [13] and Boeing 787-10 [14], which have been certified by the FAA with explicit reference to the use of onboard active control systems to ensure sufficient damping margins. Moreover, for the former aircraft, to account for potential failures of Active Modal Suppression system (called F0VMS), the rejection curve from Figure 2 was modified as reported in Figure 3. The initial requirement of minimum damping margin is lowered to 0.015 in case of inoperative control systems.

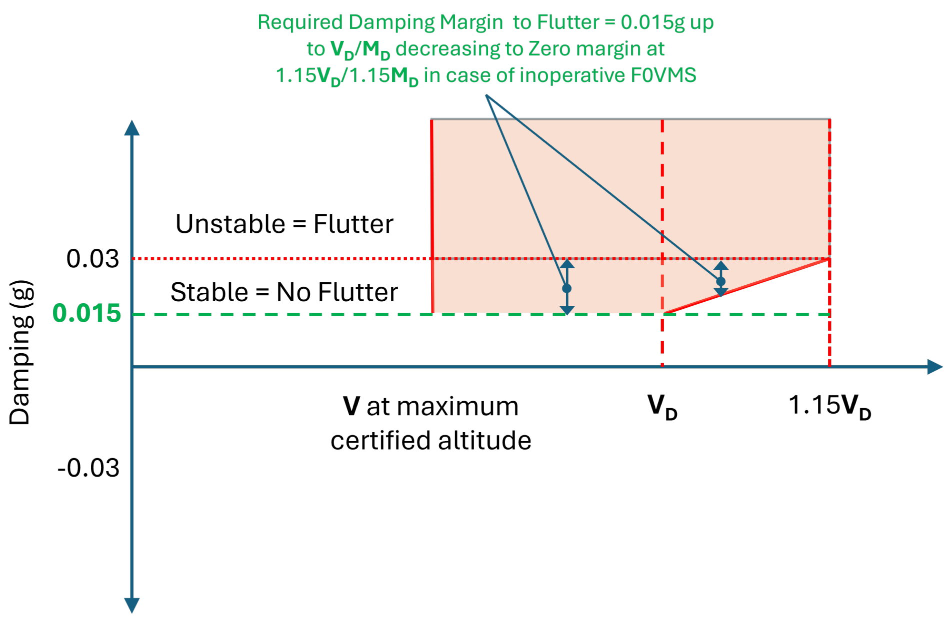

Figure 3: Method 1 for inoperative F0VMS - flutter requirements in shaded region

For the two examples, flutter-related issues emerged during the certification phase, when design modifications were no longer feasible. As often occurs, such phenomena are case-dependent and cannot be generalized. However, these instances have reignited interest in the feasibility and benefits of certifying aircrafts that meet flutter requirements using active control systems.

From a design perspective, the key question is how much structural weight savings can be achieved by leveraging existing onboard control systems to ensure compliance with flutter certification requirements while maintaining adequate safety margins. This remains an open debate, which has led to extensive specialized literature, dedicated research projects, and focused discussions at industry conferences.

The authors want to stress that this article does not aim to provide definitive answers to these complex questions, but rather contribute to the discussion with a specific case study. In particular, the work does not focus on the development of an active control system to guarantee stability, but instead seeks to quantify the potential structural weight savings associated with such an approach.

4 MODEL DESCRIPTION

The aircraft considered in the present work has been obtained in [21] starting from the publicly available data of the Airbus A330-300, whose three views are reported in Figure 4.

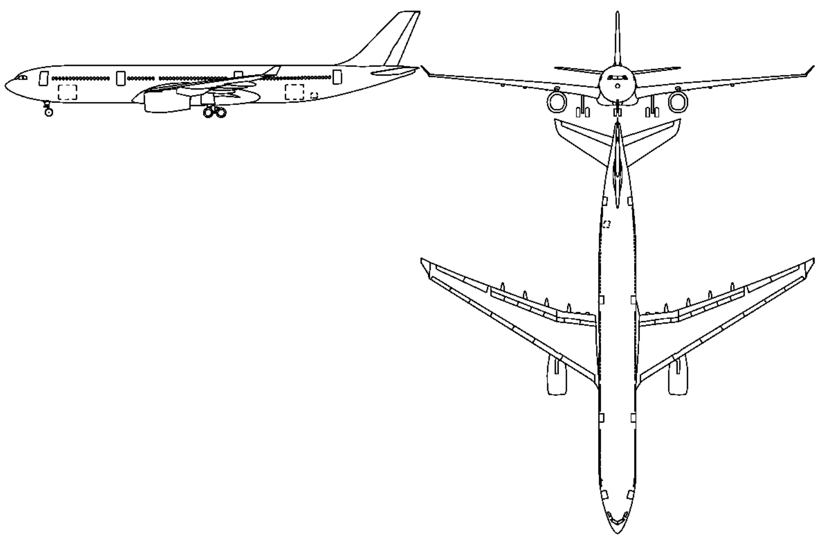

Figure 4: Views of A330-300 [21]

Since some changes have been included to produce the studied model, to avoid any confusion between the reference aircraft (A330-300) and the final one, the latter has been renamed Twin-Aisle Long-Haul (TALH) transport aircraft - from now on, simply TALH. In particular, the geometrical updates considered while creating the TALH model in AcBuilder concern wing aspect ratio, which has been increased to create a HARW. Table 1 summarizes the main requirements for such aircraft.

Table 1: TALH main requirements

Number of passengers	300 [-]
Wing Area	366.7 [m^2]
Wing Span	67 [m]
Wing Aspect Ratio	12.24 [-]
Max range	10200 [km]
Max cruise altitude	13100 [m]
Max Operating Mach number	0.87
Max Operating Speed (EAS)	175 [m/s]
Cruise speed at FL 380 (TAS)	244.91 [m/s]
Cruise speed (EAS)	127.5 [m/s]
Max lift coefficient in take-off configuration	2.1 [-]
Max lift coefficient in landing configuration	2.5 [-]
Max lift coefficient in clean wing configuration	1.75 [-]
Clean lift curve slope	5.7 [1/rad]

Recalling that GUESS allows to consider only isotropic materials, the entire model was firstly made of aluminum alloy, with the properties reported in Table 2.

Table 2: TALH material properties for GUESS sizing

Material	$E_{11,22}$ [GPa]	G_{12} [GPa]	ν_{12} [-]	ρ [kg/m^3]	σ_{max} [MPa]
AL7075-T6	72	27.69	0.3	2800	430

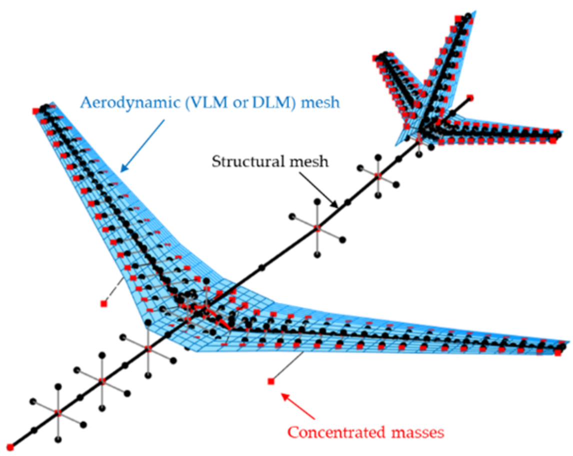

Figure 5: TALH model in NeoCASS

Starting from the requirements defined in Table 1, the entire set of manoeuvres compliant with the CS-25 regulations have been derived (Table 3) and used to generate the sized model. Figure 5 shows NeoCASS stick model, in conjunction with aerodynamic panels in correspondence of the lifting surfaces. Additionally, also the concentrated masses representing the engines are reported.

Table 3: Database of sizing manoeuvers compliant with CS25 regulations

ID	Type	N	z [m]	Mach
1-4	Pull-up	2.5	0/8061/ 0/12250	0.514/0.87/ 0.375/0.87
5-8	Push-down	-1.0	0/8061/ 0/12250	0.514/0.87/ 0.375/0.87
9	Flap max down	2.0	0	0.329
10	Static Gust for landing configuration	1.0	0	0.329
11-16	Aft movement of pitch control at VA, VC, VD URDD5 (positive and negative)	1.0	0	0.357/0.357/ 0.514
17/20/ 23/26	Sideslipe max rudder (positive and negative)	1.0	0	0.357/0.226
18/21/ 24/27	Sideslipe overswing (positive and negative)	1.0	0	0.357/0.226
19/22/ 25/28	Sideslipe maneuver 15° (positive and negative)	1.0	0	0.357/0.226
29/31	Aileron abrupt maximum deflection at VA $=\sqrt{\mathrm{N}_{max}}*$VS (positive and negative)	1.0	0	0.357
30/32	Aileron abrupt deflection + 2/3 max load factor (positive and negative)	1.7	0	0.357

Once obtained the sized model with NeoCASS, it is possible to proceed with NeOPT. In particular, NeOPT just focuses on the wing, meaning that the optimization problem will just update the structural thicknesses of that component.

5 MDO PROBLEM DEFINITION

The optimization problem solved in NeOPT can be represented as follows:

$$\min_{x \in S} f(x), S = \{x \in \mathbb{R}^{\kappa}, g(x) < 0 \cap x_{lb} \leq x \leq x_{ub}\}$$

which reads "find the design variables x belonging to the space S, that minimize the objective function $f(x)$, such that the constraints $g(x)$ are satisfied and the design variables x stay between the lower and upper bounds".

Let's define the design variables, the objective function and the constraints for the problem at hand.

5.1 Design variables

It has been anticipated that through NeOPT one can overcome the simplifications of having a symmetric isotropic wing cross-section. This is possible thanks to a 2D cross-sectional solver that provides the 6x6 beam stiffness matrix for any empty section composed of isotropic or orthotropic material. In particular, depending on the cross-section description chosen by the user, the matrices will be fully-populated, accounting for different couplings. As reported in Figure 6, the section is represented, accordingly to the semimonocoque theory, as the combination of stringers, spar caps, skins and webs (spars).

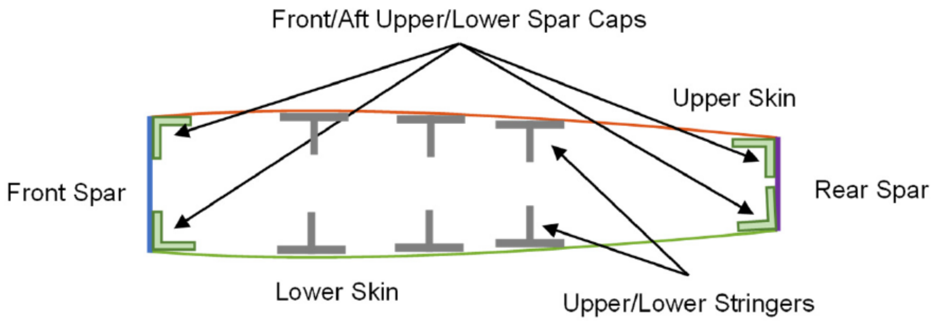

Figure 6: NeOPT cross-section description [21]

The design variables of the optimization problem, i.e. the unknowns that are determined once the problem reaches convergence, are the thicknesses of these elements. In the most general case, they are free to change independently, leading to 10 design variables per section: upper and lower stringer thickness (1-2), upper and lower front and rear spar caps thickness (3-4-5-6), upper and lower skin thickness (7-8), front and rear web thickness (9-10).

It is possible to reduce the number of unknowns by expliciting a sectional variable linking. In the case of the present study, for instance, just 7 design variables have been chosen to describe each wing section, because all the spar caps have been considered to have the same thickness. Moreover, for what concerns the material, aluminum has been substituted by composite with the stacking sequence reported in Figure 7 and the Carbon Fiber Uni-Directional (CFUD) properties reported in Table 4.

Table 4: TALH wing Carbon Fiber Uni-Directional properties

Material	E_{11} [GPa]	E_{22} [GPa]	G_{12} [GPa]	ν_{12} [-]	ρ [kg/m^3]	σ_{max} [MPa]
CFUD	135	10	5	0.3	1500	1500

The second variable linking that is computed is spanwise. Indeed, the code requires the user to provide informations on the wing spanwise description too. In this way, it is possible to divide the component in patches, assigning to each finite element that falls inside a patch the very same section description. As one can see from Figure 8, in this case 5 patches have been selected, leading to a total of 7x5=35 design variables.

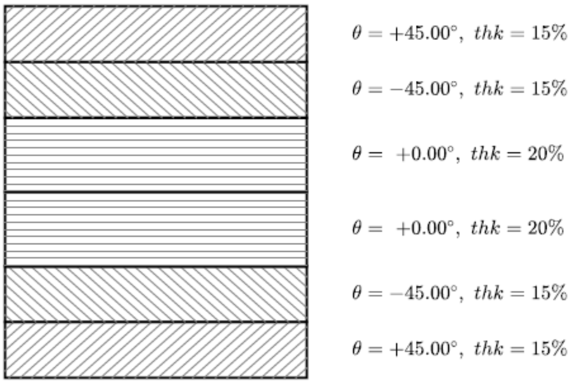

Figure 7: TALH wing composite stacking sequence

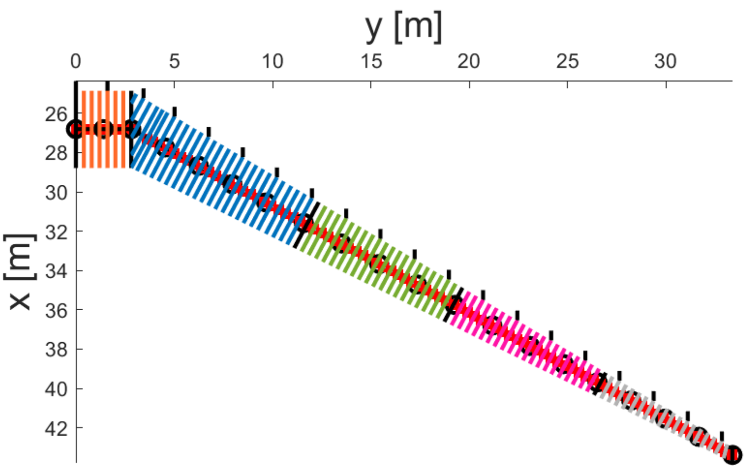

Figure 8: TALH wing patches

5.2 Objective function and constraints

As reported at the beginning of this section, the optimization problem solved in NeOPT is a minimization. The objective function is the weight of the semi-wingbox. The code, indeed, allows to just work on half wing, thanks to model symmetry. In the end, the obtained converged value can be compared either to the starting one, or to other optimization solutions, as it will be the present case.

For what concerns the constraints, two categories have been considered:

- strength requirements, i.e. no failure nor buckling;
- no flutter inside the flight envelope.

To satisfy the former set, aeroelastic trim analyses are computed in the flight conditions used to previously size the model, i.e. the ones reported in Table 3. The internal loads, and hence the stresses, are evaluated in each section component, multiplied by a safety factor of 1.5 and compared to the critical values. Tsai-Hill criterion is used for failure considerations. Once the iterative process is completed, if no local optimum is found, the code prints some informations concerning maxima constraint violations in terms of manoeuvre ID, failure or buckling, and the location at which it occurs, such that the user knows which are the weakest spots on the wing and the associated most critical manoeuvres.

Flutter constraint has been included computing a linear flutter analysis, by means of continuation method, at the corner point (z=8061 [m], Mach=0.87), requiring that for each tracked mode the maximum allowable damping was $g<0$, up to V_D, complying with the requirements represented in Figure 2. Actually, Method 1 requires to guarantee the absence of flutter up to a velocity of 1.15 V_D. However, this condition translates into a Mach number very close to 1, which poses a limit for DLM - the method used to solve aerodynamics. It has thus been chosen to not rely on aerodynamic loads that were too close to Mach=1, limiting the flutter requirements just to dive condition, without any safety margin.

5.3 Optimization problems

Since the aim of the present work is to estimate what happens in terms of mass when either flutter is explicitly excluded from the flight envelope through a passive approach, or when the structure is sized without any requirement on flutter, knowing that it can be treated *a posteriori* by means of active control systems, two different optimization problems have been solved.

- Optimization 1: failure and buckling constraints. If flutter would occur, it would be taken care of by active control systems.
- Optimization 2: failure, buckling and flutter constraints included in the problem.

The two objective functions can be compared to derive some conclusions on how treating flutter by means of passive or active approach may affect structural sizing.

6 RESULTS

6.1 Optimization 1: failure and buckling constraints

Figure 9 shows the resulting design variables for the first optimization, where only strength constraints have been considered. The initial solution has been generated adapting the semi-wingbox preliminary sizing, produced by GUESS, to the new wingbox description of NeOPT, updating the material and including the variable linking.

Looking at the web thicknesses, one can notice that the initial solution produced an unrealistic value in correspondence of the fourth patch. This can be easily solved by the optimization process, which ensures not only the satisfaction of the constraints, but also that the design variables fall between lower and upper bounds defined by the user.

In terms of masses, a comparison between the initial and the optimized solutions is given in Table 5.

Figure 10 shows a comparison between the initial and the optimized models root loci, computed at z=8061 [m] and V_D, to keep Mach<1. As one can notice, the initial model does not present flutter, while this occurs for the optimized one. This is not a surprise, considering that the optimization problem has been defined without taking care of flutter, and hence accepting that it could have fallen inside the envelope.

Table 5: TALH semi-wingbox results - Optimization 1

	Initial	Final	Δ
Semi-wingbox Mass	24795.31 [kg]	6417.27 [kg]	-74%

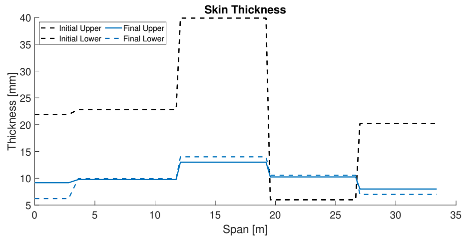

(a) Skins

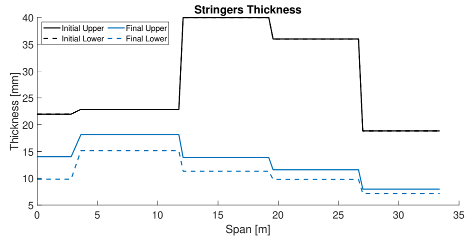

(b) Stringers

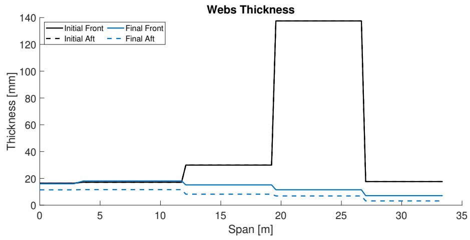

(c) Webs

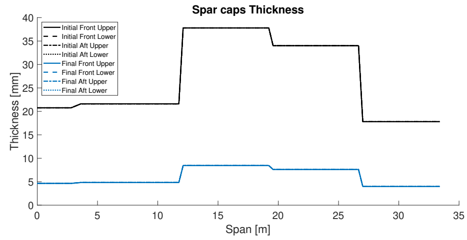

(d) Sparcaps

Figure 9: TALH thicknesses - Optimization 1

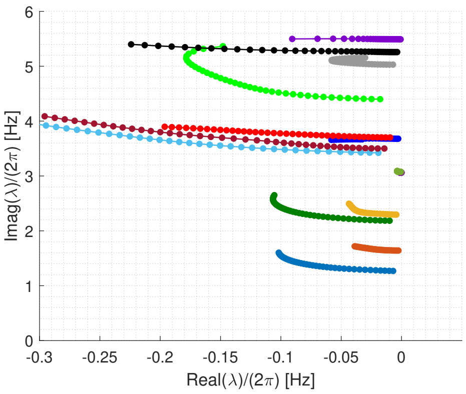

(a) Initial

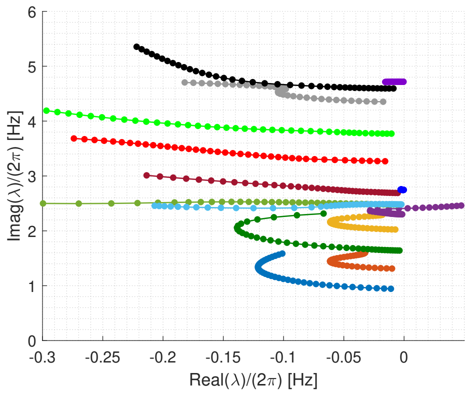

(b) Final

Figure 10: TALH root loci - Optimization 1

To characterize the mechanism, V-f and V-g plots are reported in Figure 11 for the optimized model, isolating the modes that are closer to flutter frequency. The coalescing modes are the fifth and the sixth deformable ones. In both subfigures the lines correspondent to V_D and 1.15 V_D have been reported highlighting the limits that must be considered from the regulatory point of view. Moreover, in the subfigure of damping also an horizontal line correspondent to g<0.03 (or ξ <0.015) has been added to delimit the region of unstable flutter accordingly to Figure 2. In this optimization no active control system was implemented yet to counteract flutter.

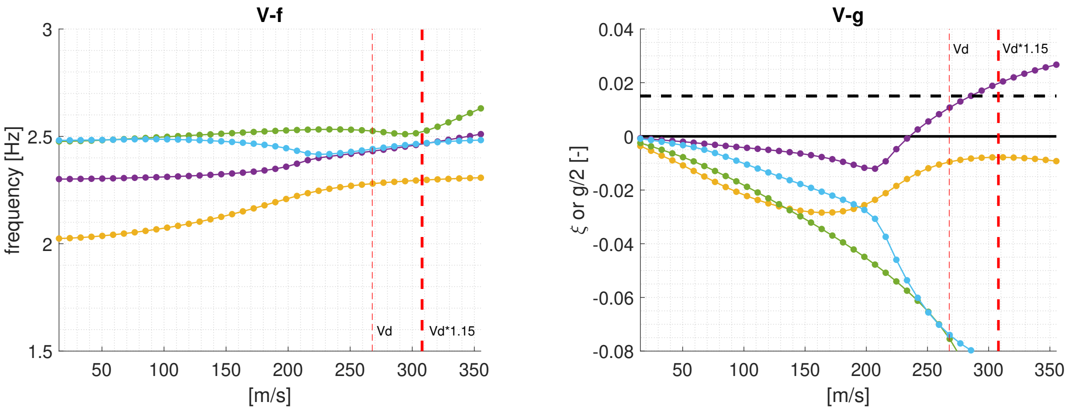

(a) Frequency (b) Damping

Figure 11: TALH V-f and V-g - Optimization 1

To further investigate the phenomenon, one can look at the resulting flutter mode, which is shown in Figure 12. It is given by an interaction between inplane and out-of-plane wing symmetric bending and wing symmetric torsion. However, looking at the tail plane, it seems that a participation of the horizontal tail and the fuselage are also present. Since NeOPT acts only on the wing, if an AFS system would be designed and included inside the aero-servo-elastic optimization, it could occur that flutter won't be canceled, due to the uncontrollable participation of fuselage and tail. This issue has not been addressed yet and will be treated in future works.

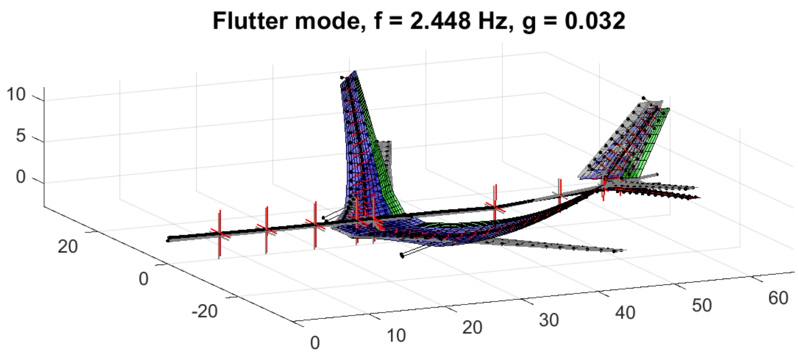

Figure 12: TALH flutter mode - Optimization 1

6.2 Optimization 2: failure, buckling and flutter constraints

For the second problem, also the flutter constraint has been included inside the optimization, leading to the results shown in Figure 13.

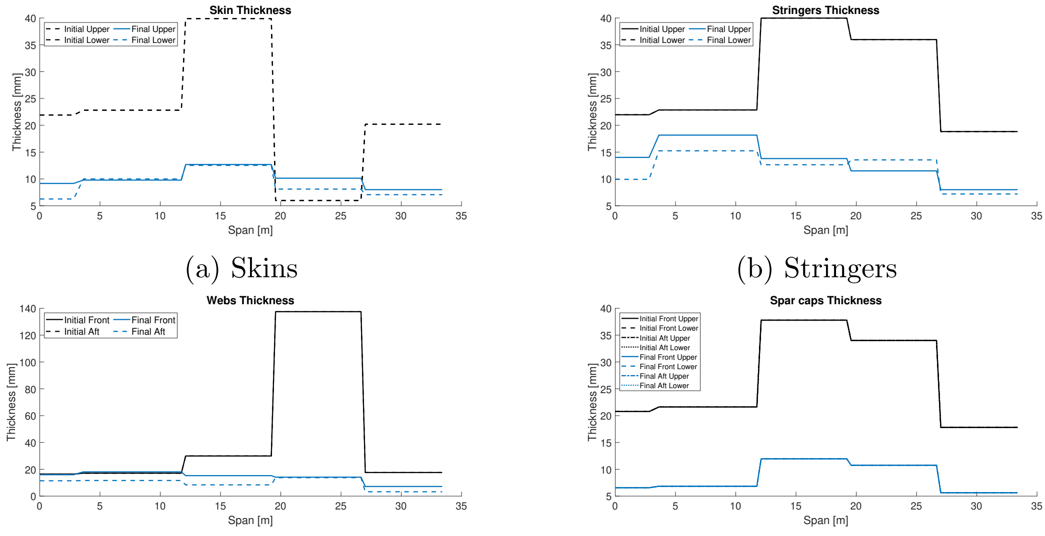

(a) Skins (b) Stringers

(c) Webs (d) Sparcaps

Figure 13: TALH thicknesses - Optimization 2

Table 6 contains the results in terms of sizing. As one can notice, the final mass, i.e. the one of the optimized model, is higher in this case with respect to what has been obtained from the first optimization.

Table 6: TALH semi-wingbox results - Optimization 2

	Initial	Final	Δ
Semi-wingbox Mass	24795.31 [kg]	6676.83 [kg]	-73%

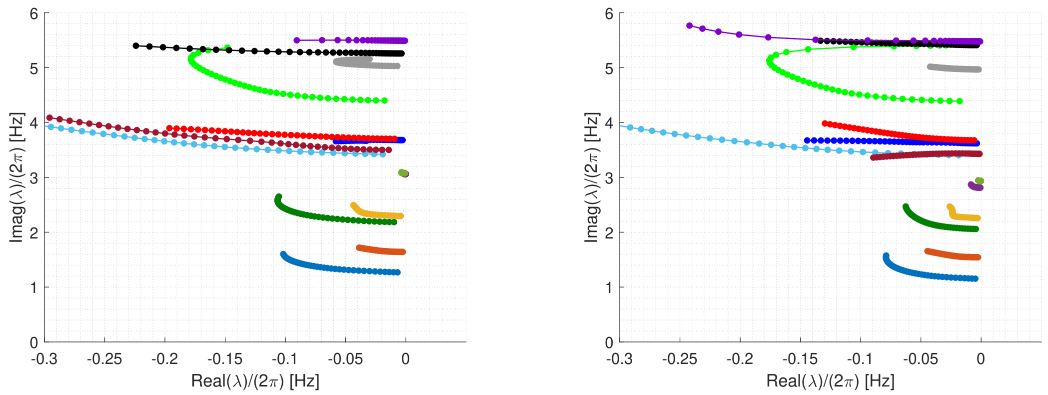

(a) Initial (b) Final

Figure 14: TALH root loci - Optimization 2

For what concerns flutter analysis, simply by looking at the root loci, computed also in this case at z=8061 [m] and V_D, one can notice that no flutter occurs, as shown in Figure 14.

For sake of completeness, also the V-g plots for both the initial and the optimized model are reported in Figure 15, including all the deformable modes to be tracked, to show that none of them crosses the flutter constraint line.

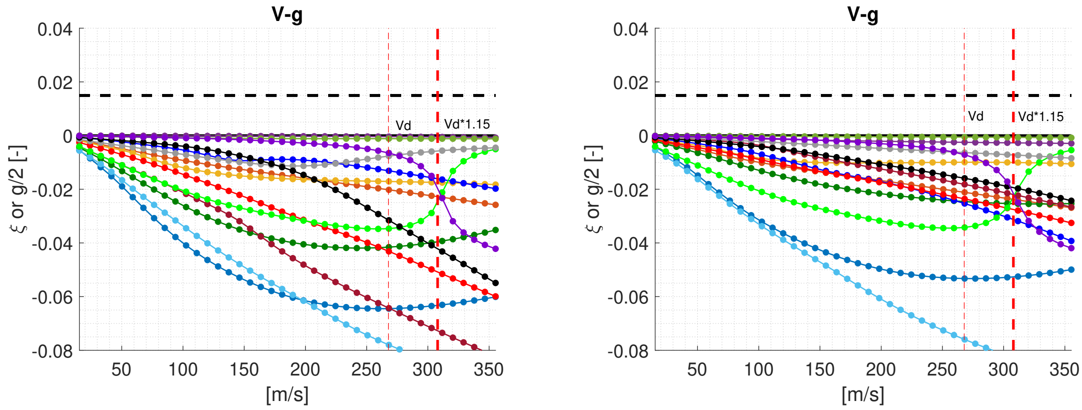

(a) Initial (b) Final

Figure 15: TALH V-g plot - Optimization 2

6.3 Sizing results comparison

A comparison of sizing results in terms of thicknesses and semi-wingbox mass is reported in Figure 16 and Table 7, respectively. Not including flutter constraint inside the optimization process leads to a mass gain of around 200 [kg] - 3.9% - per half wing.

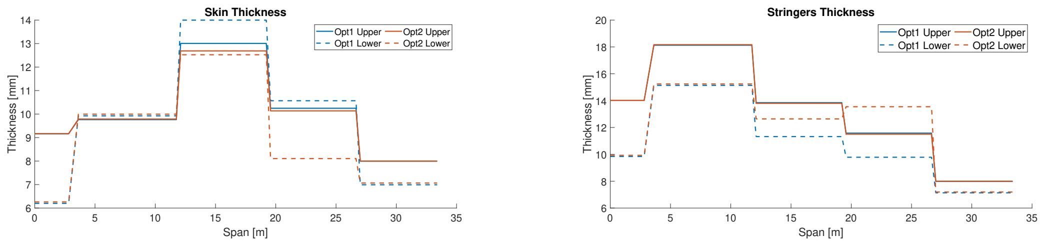

(a) Skins (b) Stringers

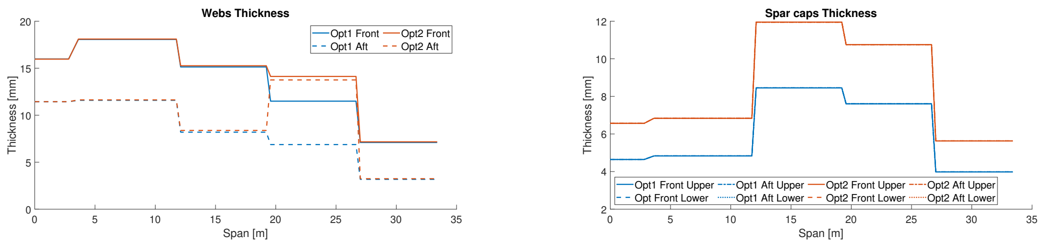

(c) Webs (d) Sparcaps

Figure 16: TALH results comparison

Table 7: TALH semi-wingbox results comparison

	Optimization 1	Optimization 2	Δ
Semi-wingbox Mass	6417.27 [kg]	6676.83 [kg]	+3.88%

7 CONCLUSIONS

Flutter is one of the most dangerous phenomena that an aircraft can experience. For safety reasons, aircrafts are required to prove flutter-freedom throughout the entire flight envelope, with a due safety margin. Despite the effectiveness of using Active Flutter Suppression systems to manage flutter, as demonstrated by the vast literature, this option has not been supported by certification rules. However, two recent cases highlight certification possibilities with active control systems, sparking new discussions on studying and enhancing such systems.

From a structural standpoint, this means taking advantage of the many active control systems already present in future aircraft to control flutter and simultaneously reduce structural weight, aligning with modern efforts to reduce emissions. While flutter is case-dependent, making it difficult to derive a general rule, this paper attempts to quantify the potential structural weight advantage in the analyzed case if the flutter constraint is considered from the beginning of the design process, allowing active control systems to handle flutter suppression. Two optimization problems were solved using the coupling of NeoCASS and NeOPT, explicitly including or excluding the flutter constraint. The results indicate a potential reduction in wingbox mass of around 200 [kg] per semi-wingbox. This weight advantage needs to be weighed against the mass of new control systems required to implement the AFS functionality. Additionally, issues related to reliability and safety aspects must be addressed to complete the certification process.

ACKNOWLEDGEMENTS

The U-HARWARD Project has received funding from the Clean Sky 2 Joint Undertaking, under the European's Union Horizon 2020 research and innovation Program under Grant Agreement number: 886552-H2020-CS2-CFP10-2019-01. The content of this document reflects only the author's view. The European Commission and Clean Sky 2 Joint Undertaking (CS2JU) are not responsible for any use that may be made of the information it contains.

REFERENCES

[1] R. L. Bisplinghoff, H. Ashley, and R. L. Halfman. *Aeroelasticity*. Dover Publications, Mineola, NY, 2 edition, 1996.

[2] M. M. Opgenoord, M. Drela, and K. M. Willcox. Influence of Transonic Flutter on the Conceptual Design of Next-Generation Transport Aircraft. In *AIAA/ASCE/AHS/ASC Structures, Structural Dynamics, and Materials Conference*, Kissimmee, FL, 2018. doi:10.2514/6.0948.

[3] E. Livne. Future of Airplane Aeroelasticity. *Journal of Aircraft*, 40(6):1066–1092, 2003. doi:10.2514/2.7218.

[4] E. Garrigues. A Review of Industrial Aeroelasticity Practices at Dassault Aviation for Military Aircraft and Business Jets. *Aerospace Lab*, 14:1–34, 2018. doi:10.12762/2018.AL14-09.

[5] J. R. Martins and A. B. Lambe. Multidisciplinary Design Optimization: A Survey of Architectures. *AIAA Journal*, 51(9):2049–2075, 2013. doi:10.2514/1.J051895.

[6] Z. Lyu, G. K. W. Kenway, and J. Martins. Aerodynamic Shape Optimization Investigations of the Common Research Model Wing Benchmark. *AIAA Journal*, 53(4): 968–985, 2015. doi:10.2514/1.J053318.

[7] G. Dimitriadis. *Introduction to Nonlinear Aeroelasticity*. John Wiley and Sons, 2017. doi:10.1002/9781118756478.

[8] B. Stanford and P. Beran. Direct Flutter and Limit Cycle Computations of Highly Flexible Wings for Efficient Analysis and Optimization. *Journal of Fluids and Structures*, 36:111–123, 2013. doi:10.1016/j.jfluidstructs.2012.08.008.

[9] G. J. Kennedy, G. K. W. Kenway, and J. Martins. Towards Gradient-Based Design Optimization of Flexible Transport Aircraft with Flutter Constraints. In *15th AIAA/ISSMO Multidisciplinary Analysis and Optimization Conference*, Atlanta, GA, 2014. doi:10.2514/6.2726.

[10] E. Jonsson, C. Rico, C. Lupp, C. Cesnik, and R. Martins, Joaquim. Flutter and Post-Flutter Constraints in Aircraft Design Optimization. *Progress in Aerospace Sciences*, 109:100537, 2019.

[11] E. Livne. Aircraft Active Flutter Suppression: State of the Art and Technology Maturation Needs. *Journal of Aircraft*, 55(1):410–452, 2017. doi:10.2514/1.C034442.

[12] C. Cesnik, R. Palacios, and E. Reichenbach. Reexamined Structural Design Procedures for Very Flexible Aircraft. *Journal of Aircraft*, 51(5):1580–1591, 2014. doi:10.2514/1.C032464.

[13] Proposed Special Condition for Installation of Flutter Suppression System Applicable to Boeing B 747-8F/-8.

[14] Special Condition on Flaps-Up Vertical Modal-Suppression System Applicable to Boeing 787-10. URL `https://www.easa.europa.eu/en/downloads/23783/en`.

[15] L. Cavagna, S. Ricci, and L. Travaglini. NeoCASS: An Integrated Tool for Structural Sizing, Aeroelastic Analysis and MDO at Conceptual Design level, 2011. ISSN 03760421.

[16] L. Cavagna, S. Ricci, and L. Riccobene. Structural Sizing, Aeroelastic Analysis, and Optimization in Aircraft Conceptual Design. *Journal of Aircraft*, 48:1840–1855, 2011. ISSN 0021-8669. doi:10.2514/1.C031072.

[17] L. Cavagna, S. Ricci, and L. Travaglini. Aeroelastic Analysis and Optimization at Conceptual Design Level Using NeoCASS Suite. In *Collection of Technical Papers - AIAA/ASME/ASCE/AHS/ASC Structures, Structural Dynamics and Materials Conference*, 2011. doi:10.2514/6.2011-2079.

[18] EASA. Certification Specifications for Large Aeroplanes CS25, 2024. URL https://www.easa.europa.eu/en/document-library/certification-specifications/group/cs-25-large-aeroplanes.

[19] EASA. CS-23 Normal, Utility, Aerobatic and Commuter Aeroplanes, 2025. URL https://www.easa.europa.eu/en/document-library/certification-specifications/group/cs-25-large-aeroplanes.

[20] F. Toffol and S. Ricci. A Meta-Model for Composite Wingbox Sizing in Aircraft Conceptual Design. *Composite Structures*, 306, 2023. ISSN 02638223. doi:10.1016/j.compstruct.2022.116557.

[21] F. Toffol and S. Ricci. Preliminary Aero-Elastic Optimization of a Twin-Aisle Long-Haul Aircraft with Increased Aspect Ratio. *Aerospace*, 10(4), 2023. ISSN 22264310. doi:10.3390/aerospace10040374.

[22] Federal Aviation Administration. AC 25.629-1B - Aeroelastic Stability Substantiation of Transport Category Airplanes. 10 2014. URL https://www.faa.gov/documentLibrary/media/Advisory_Circular/AC_25_629-1B.pdf.

[23] A. S. Thelen, B. Stanford, and K. Jacobson. Flutter and stochastic gust constraint studies of the undeflected crm using mphys. In *AIAA Scitech 2024 Forum*, page 2774, 2024.

[24] A. Lunghitano, F. Afonso, and A. Suleman. A study on the surrogate-based optimization of flexible wings considering a flutter constraint. *Applied Sciences*, 14(6): 2384, 2024.